remote sensing

MDPI

Article

Changes in Land Use and Ecosystem Service Values of Dunhuang Oasis from 1990 to 2030

Fan Yi [1,2,3,†], Qiankun Yang [1,2,3,†], Zhongjing Wang [4,5], Yonghua Li [1,2,3], Leilei Cheng [1,2,3], Bin Yao [1,2,3] and Qi Lu [1,2,3,*]

[1] Institute of Desertification Studies, Chinese Academy of Forestry, Beijing 100091, China
[2] Observation and Research Station of Dunhuang Desert Ecosystem, National Forestry and Grassland Administration, Dunhuang 736200, China
[3] Observation and Research Station of Kumtag Desert, National Forestry and Grassland Administration, Dunhuang 736200, China
[4] State Key Lab of Hydroscience and Engineering, Department of Hydraulic Engineering, Tsinghua University, Beijing 100084, China
[5] Breeding Base for State Key Laboratory of Land Degradation and Ecological Restoration in Northwest China, Ningxia University, Yinchuan 750102, China
* Correspondence: luqi@caf.ac.cn; Tel.: +86-139-1083-0860
† These authors contributed equally to this work.

Abstract: Maintaining the integrity and stability of oasis ecosystems is an important topic in the field of ecological research. Assessment of ecosystem services and their changes can provide important support for the sustainable development of oases. This study took the Dunhuang oasis in the hyper-arid area as the research object and used 1990, 2010, and 2020 Landsat series satellite images to complete the land use interpretation by random forest classification. Then we estimated the ecosystem services value (ESV) by using benefit transfer method, and predicted the trend of ecosystem service value changes under three scenarios using the Analytic Hierarchy Process method and the patch generation land use simulation model (AHP-PLUS model). The results showed that the vegetation areas of the Dunhuang Oasis first decreased and then increased during 1990–2020. The decrease was largely due to the expansion of built-up land and farmland, and the increase was mainly contributed by the implementation of ecological protection policies. The path of changes in the ESV of the Dunhuang Oasis during 1990–2020 was well consistent with that of vegetation areas, with a maximum of 9068.15×10^6 yuan (in 1990) and a minimum of 6271.46×10^6 yuan (in 2010). Spatial autocorrelation analysis showed that urbanization reduced ESV, and the implementation of ecological policies enhanced ESV. The ESV of the Dunhuang Oasis for the year 2030 under the ecological conservation scenario could reach 7631.07×10^6 yuan, which is 381.1×10^6 yuan higher that under the economic development scenario. The ecological conservation scenario is the optimal option to achieve sustainable development of the Dunhuang Oasis. We suggested that the government should continuously enhance the protection of forests and waterbodies, reasonably restrict production and domestic water consumption, and efficiently increase the proportion of ecological water consumption. In addition, this study improved the evaluation method of oasis ESV based on the proportion of Normalized Difference Vegetation Index (NDVI) of grasslands with different coverage, which is important for improving the environment in arid areas.

Keywords: ecosystem service value; land cover change; land use simulation; hyperarid area oasis

Citation: Yi, F.; Yang, Q.; Wang, Z.; Li, Y.; Cheng, L.; Yao, B.; Lu, Q. Changes in Land Use/Cover and Ecosystem Service Values of Dunhuang Oasis from 1990 to 2030. *Remote Sens.* **2023**, *15*, 564. https://doi.org/10.3390/rs15030564

Academic Editor: Conghe Song

Received: 30 October 2022
Revised: 23 December 2022
Accepted: 5 January 2023
Published: 17 January 2023

1. Introduction

Ecosystem service value (ESV) has gained widespread attention as a tool to assess the interrelationship between human economic society and natural ecosystems [1,2]. Ecosystem services are the obvious or potential benefits that people receive from ecosystems, and the main indicators include supply services, regulatory services, support services, and cultural services [3–6]. The accurate evaluation of ESV provides important information for the development of reasonable ecological conservation policy [7]. Previously researchers worked on ecosystem service assessment from several perspectives, but the early research was qualitative in nature and did not provide a reasonable ESV quantification method, limiting the attention and support the research received from international organizations and national governments [8–10]. Until 1984 Kellert [11] applied the profit-and-loss approach to assessments of wildlife and environmental resources, pioneering a new framework of standardization-quantification-assessment of biosphere materials. In conjunction with Kellert's findings, Constanza et al. [12] proposed the benefit transfer approach based on the relationship between ecosystem services and functions and valued 17 ecosystem services in the global biosphere, attracting widespread attention from scholars. The benefit transfer method argues that the actual economic value of ecosystem services depends on the interaction between ecosystem supply and social demand [13]. It assumes that the monetary valuation of the importance of ecosystem services to society can establish a system for quantifying the value of services of different ecosystems; in addition, the monetary valuation results can be easily incorporated into the national economic accounting system to support the decision-making of government departments. However, the limitations of the benefit transfer method are as follows: (1) the determination of value coefficients is subjective to some extent [14–16], and (2) whether the value coefficients are consistent with the actual situation of the study area will directly affect the accuracy of the assessment [5]. To address this issue, Xie et al. [17–20] developed a revised coefficient table applicable to China based on the characteristics of terrestrial ecosystems. The improved method has the advantages of low data acquisition cost and a simple evaluation process, and has been widely used by Chinese researchers [21–23].

According to the Millennium Ecosystem Assessment (MA), nearly 60% of ecosystems are in a degraded state, and the main cause is land use change (LUCC) due to human activities [24]. Dynamics in land use patterns lead to changes in the area and spatial distribution of different ecosystem types, which in turn affect the types and intensity of ecosystem services [25,26]. Therefore, the process and mechanism of interaction and synergistic evolution between land use change and ESV are the focus of current research. Researchers usually use the information on the land use, population, and economy of the study area to investigate the relationship between land use change and ESV through spatiotemporal analysis. For example, Wang et al. [27] showed that the ESV loss in the Guangdong-Hong Kong-Macao Greater Bay Area due to urban expansion amounted to 40.5 billion RMB, of which the reduction on waterbodies was the main cause. Dai et al. [28] quantitatively assessed the ESV from the perspective of natural and social ecology in ESV in Chengdu, China, and found that population and Gross Domestic Product (GDP) growth due to the increased urbanization rate was the main reason for ESV decline. ESV-related studies have mainly focused on developed cities with frequent land use changes, high population density, and complete records of social statistics. In recent years, with the improvement of ESV assessment methods, some researchers have begun to focus on arid areas with low population density, little available data information, and very fragile ecosystems [29–31].

Oases are the main living area for humans in arid areas, and, as such, they assume important ecosystem service functions. The United Nations Convention to Combat Desertification (UNCCD) reported that land use changes in oasis cities have significantly reduced the quality and/or quantity of ecosystem services [32]. Maimaiti et al. [31] assessed the ESV of oasis cities in the Tarim Basin and found that the ESV in the region decreased at a rate of 21.54% during the period from 1990 to 2015 and that urban expansion was the

main cause of this phenomenon. Zhang et al. [33] assessed the ESV spatio-temporal dynamics of ESV in hyperarid area and found that the degradation of water bodies into saline-alkali land was the main reason for the decline of ESV. Tan et al. [34] reported a significant decline in the ESV of the Zhangye Oasis before 2000 due to the severe destruction of forests, grasslands, and wetlands; after 2000, the ESV began to recover due to the implementation of a series of ecological projects.

Several ecological conservation projects implemented by the Chinese government in recent years have contributed to the recovery of ESV in some oasis cities, and whether the recovery trend is sustainable in the future is a key question [35]. In previous studies, researchers most assessed present or past ESV, and few predictions of future ESV sustainability have been presented. This study uses the 106 Patch generation Land Use Simulation model (PLUS) to predict ESV, and combines Ana- 107 lytic Hierarchy Process method (AHP) method to improve the objectivity of the prediction results; In addition, previous studies have shown that grassland is the main land type contributing to ESV in arid areas, but few researchers have made a more refined evaluation of grassland ESV [36,37]. Based on the difference characteristics of Normalized Difference Vegetation Index (NDVI) values of grasslands with different coverage, this study calculated the ESV equivalent values of three grasslands with different coverage by ratio method, and developed an evaluation model of oasis ESV in arid areas focusing on grassland. Based on the above methods, this study made a more detailed assessment and prediction of the ESV of Dunhuang Oasis from 1990 to 2030, providing decision-making suggestions for regional ecological protection and land use planning.

2. Materials and Methods

2.1. Study Area Overview

Dunhuang Oasis is located at the westernmost end of Hexi Corridor (39°50′50″-40°36′54″N, 93°44′35″- 95°31′55″E). With an average elevation of 1138 meters, annual average precipitation of 44.8 mm, evaporation of 2128.7 mm, and an annual average temperature of 10.7℃ (Figure 1). It is a typical oasis in an extremely arid area, surrounded by desert and Gobi, and is short of water resources. Danghe River and Shule River are distributed in the territory, and the main water source is supplied by the Danghe River. Since the 1990s, the Shule River has dried up, the population in the oasis has increased rapidly, and the degree of desertification has become increasingly serious, which seriously threatens the ecological security of the oasis.

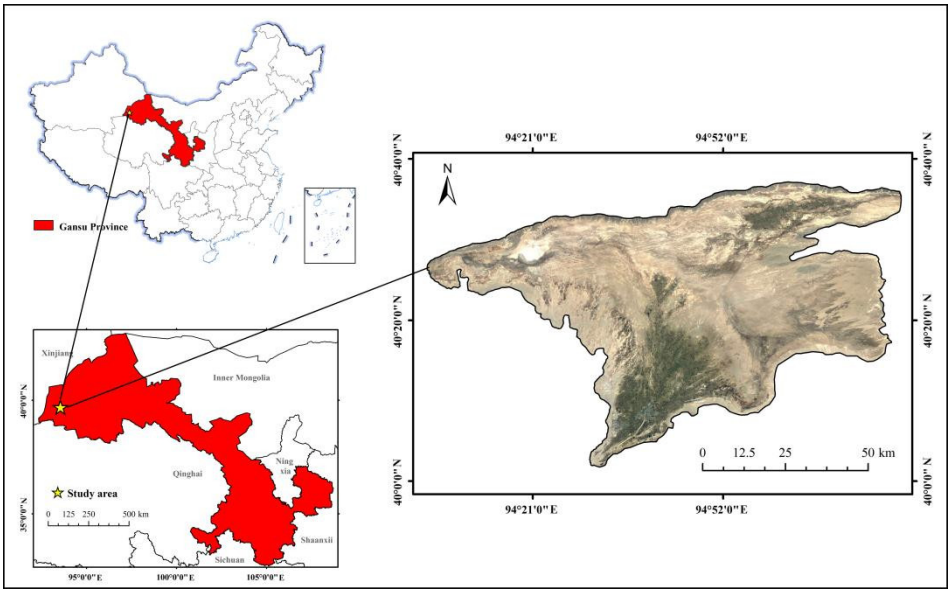

Figure 1. Geographic of the study area.

2.2. Data preparation

In the study, three physical geographical factors (temperature, elevation, and slope) and five social and economic factors (distance to farmland, roads and residential areas, GDP and population density) were collected. Digital elevation model (DEM) data (30×30m) 134 was obtained from the Geospatial Data Cloud (http://www.gscloud.cn, accessed on 25 March 2022); slope data were calculated from DEM data by arcgis10.6; land surface temperature and farmland data were calculated from Landsat images by ENVI5.3. Population density raster data (1 × 1 km) were procured from World Population (https://www.worldpop.org, accessed on 25 March 2022). GDP raster data (1 × 1 km) was obtained from the National Earth System Science Data Center, National Science & Technology Infrastructure of China (http://www.geodata.cn, accessed on 27 March 2022). Residential raster data (30 × 30 m) was obtained from the Resources and Environment Science and Data Center (https://www.resdc.cn/Default.aspx, accessed on 27 March 2022). Road data (30 × 30 m) were procured from Open Street Map (https://www.openstreetmap.org, accessed on 27 March 2022). All data were resampled to 30 m resolution for calculations. Extracting the distance to farmland, road and residential by Euclidean distance analysis, the social and economic data used for the assessment and analysis of ESV were from Gansu Statistical Yearbook and China Agricultural Statistical Yearbook during 1990–2020. The Landsat series images were downloaded from the United States Geological Survey (USGS) website (https://earthexplorer.usgs.gov, accessed on 07 January 2022). Image resolution was 30 m, and the time series was 1990–2020, divided into three periods (1990, 2010, 2020).

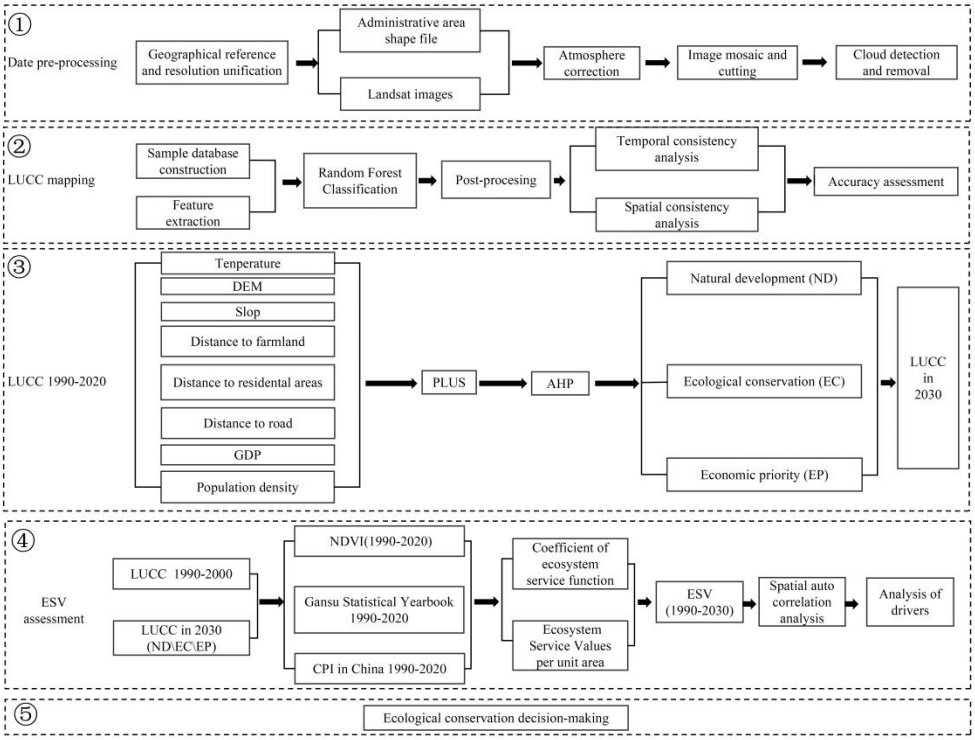

Figure 2. Framework of this study.

2.3. Data Preparation Processing

Random forest classification has the advantages of high classification accuracy, fast processing speed, and stable optimization performance of outliers and noise[38,39]. Based on the random forest classification, the land use types of Dunhuang Oasis were divided into built-up land, farmland, water body, bare land, moderate-cover grassland, high-

cover grassland, shrub forest, and broad-leaved forest. The classification results were corrected through manual visual interpretation. A total of 1000 test samples were obtained through field surveys, consultation with residents, and comparison of historical images on Google Maps, to verifiy the accuracy of classification (Figure 2).

To measure the degree of agreement, we used the overall accuracy, producer accuracy and Kappa index. The overall accuracy is the percentage of the correctly classified samples to the total number of samples, the producer accuracy is the percentage of correctly classified samples to reference data samples, and the Kappa index is calculated from the difference between the observed agreement and the expected agreement, as shown in Eqs. (1)–(3) [40]. In the classification results, the overall accuracy was over 87% and the kappa coefficients were greater than 0.81 (Appendix A, Tables A1–A3), which satisfied the practical application requirements with the substantial agreement.

$$P_O = \frac{\sum_{i=1}^{C} T_i}{n} \quad (1)$$

$$P = \frac{\sum_{i=1}^{C} a_i * b_i}{n^2} \quad (2)$$

$$K = \frac{P_O - P_e}{1 - P_e} \quad (3)$$

where, K is Kappa index; P_o is the sum of the number of correctly classified samples of each class divided by the total number of samples, that is, the overall accuracy; P_e is proportion of units for expected change agreement; C is the total number of categories; and T_i is the number of samples correctly classified for each category; a_i is the number of real samples of each category; bi is the number of samples of classification results; and the total number of samples is n.

2.4. AHP-PLUS Model

PLUS Model

The patch generation land use simulation model (PLUS) is a future land use change simulation model that integrates the land expansion analysis strategy (LEAS) module and the cellular automata (CA) model based on multiclass random patch seeds [41,42]. This study predicts the land use change of the Dunhuang Oasis in 2030 through the PLUS model. First, the raster data of land use types in 2000 and 2010 were inputted to obtain the data of land use type changes. Secondly, three physical geographical factors (temperature, DEM and slope) and five social and economic factors (distance to farmland, roads and residential areas, GDP and population density) were inputted to identify their driving forces. Finally, the above results were used to simulate the land use of the Dunhuang Oasis in 2020, and compared with the actual land use image, with the predicted image having a Kappa coefficient of 0.839, with an overall accuracy of 92.39%, indicating a high degree of credibility.

AHP Method

The analytic hierarchy process (AHP) method is a decision-making method that can divide the factors in a complex problem into related, hierarchically ordered, and structured categories, with the advantage of multi-objective and multi-criteria. The specific steps, are as follows: (1) Establish an ordered hierarchical model, generally divided into three categories, namely the objective layer, the criterion layer and the solution layer, with no more than nine elements dominated by each layer (Appendix A, Tables A4 and A5). (2) Construct the judgment matrix and calculate the maximum characteristic root λmax; and (3) hierarchical ranking (Pw) and consistency test (CR). When the CR of the judgment matrix P is <0.1 or λmax = n, CI = 0, P is considered to have satisfactory consistency, otherwise the elements in P need to be adjusted to make it satisfactorily consistent [43,44].

$$P_w = \lambda_{max} \tag{4}$$

$$CI = (\lambda_{\max} - n)/(n-1) \tag{5}$$

$$CR = CI/RI \tag{6}$$

where P_w is the eigenvector corresponding to the largest eigenroot of the judgment matrix; n is the order of judgment matrix; CI is the consistency index of judgment matrix; RI is the average random consistency index of the judgment matrix, and CR is the random consistency ratio of the judgment matrix.

2.5. Scenarios

In the land use change simulation research, current researchers mainly use qualitative methods to define the transfer rate of land use types [42,45]. AHP is an effective method that combines quantitative and qualitative analysis, which helps to improve the objectivity of the evaluation results. Thus, in the study, we adopt the AHP method to determine the transfer rate of different land use types, the results are as follows:

(1) Natural development (ND) scenario: Considering the urbanization process and existing land policies, the land use development trend from 2010 to 2020 is continued, and the transfer probability of each land use type remains unchanged to simulate the land use situation in 2030.

(2) Ecological conservation (EC) scenario: With ecological environmental protection as the primary purpose, the land transfer of broad-leaved forest, grassland, and waterbody is strictly restricted, and the transfer of broad-leaved forest, grassland, and waterbody to farmland and built-up lands is strictly controlled. The rate of conversion of bare land to grassland and waterbody area is increased by 57.14%, the probability of conversion of grassland to shrub forest is increased by 28.57%, and the probability of conversion of shrub forest to the broad-leaved forest is increased by 14.29%.

(3) Economic priority (EP) scenario: There is no restriction on the expansion of farmland and built-up land areas, and the probability of conversion between land area types are adjusted to increase the probability of transferring bare land, grassland, broad-leaved forest, and shrubs to farmland and built-up land areas by 57.14%, 28.57%, 14.29%, and 14.29%, respectively.

2.6. Ecosystem Service Value

The grasslands in the study area were divided into low-, moderate- and high-cover grasslands and the equivalent factors were calculated for different cover grasslands. Biomass was positively correlated with ecosystem function and NDVI was significantly and positively correlated with biomass. Therefore, we used Equations 7, and 8 to calculate the equivalence factors for low, moderate, and high-cover grasslands, and the parameters of Xie et al. [20] were used for the remainder of the land equivalence factor.

$$w = \frac{NDVI_m}{NDVI_n} \tag{7}$$

$$e_{ij} = \lambda_{ij} \times w \tag{8}$$

where, m represents the land use category of the high, medium, and low grassland, n represents the land use category of grassland, and NDVI is selected as the mean value of maximum NDVI in 2020 for the land category to which it belongs. j is the type of ecosystem service function, i is the type of land cover, and λ represents the equivalence factor of grassland (Table 1).

Table 1. Ecosystem Service Values per unit area in different Chinese land ecosystems.

Service Type		Ecosystem service value/(yuan·hm^{-2}·a^{-1})							
Categories	**Sub-Categories**	**BL**	**LCG**	**MCG**	**HCG**	**SF**	**BF**	**WB**	**FL**
Provisioning services	Food production	0.01	0.27	0.60	1.04	0.19	0.29	0.8	0.85
	Raw material production	0.03	0.40	0.88	1.53	0.43	0.66	0.23	0.4
	Water supply	0.02	0.22	0.49	0.85	0.22	0.34	8.29	0.02
Regulating services	Gas regulation	0.11	1.42	3.09	5.38	1.41	2.17	0.77	0.67
	Climate regulation	0.1	3.74	8.17	14.24	4.23	6.5	2.29	0.36
	Purify environment	0.31	1.24	2.70	4.70	1.28	1.93	5.55	0.1
	Hydrological regulation	0.21	2.75	5.99	10.44	3.35	4.74	102.24	0.27
Supporting services	Soil conservation	0.13	1.72	3.76	6.56	1.72	2.65	0.93	1.03
	Nutrient cycling	0.01	0.13	0.28	0.49	0.13	0.2	0.07	0.12
	Biodiversity	0.12	1.57	3.42	5.96	1.57	2.41	2.55	0.13
Cultural services	Aesthetic landscape	0.05	0.69	1.51	2.62	0.69	1.06	1.89	0.06

Note: BL, bare land; LCG, low-cover grassland; MCG, moderate-cover grassland; HCG, high-cover grassland; SF, shrub forest; BF, broad-leaved forest; FL, farmland.

The average annual economic value of natural grain production per unit of farmland in the Dunhuang Oasis was calculated based on the rule that "the economic value of production services provided by an existing unit of farmland is seven times the economic value of a natural ecosystem without human inputs". The Consumer Price Index (CPI) index for the period from 1990 to 2020 was selected to correct grain prices (Eq 9) [46], considering the impact of price levels and inflation on grain prices in the last three decades. Based on the corrected economic value of grain crops (wheat, corn, soybean) for the correction and calculation of their average value, the results showed that the economic value per unit of ecosystem services (E_a) in the study area was 2072.76 yuan/hm^2 (Eq 10).

$$y_n = \begin{cases} 100, & n = 1990 \\ x_n, n = 1991 \\ x_n \times \frac{y_{n-1}}{100}, n = 1992,1993 \ldots \end{cases} \quad (9)$$

$$E_a = \frac{1}{7} \times \sum_{l}^{s} m_l \, p_l q_l / M \times \frac{R}{R_0} \quad (10)$$

where x_n refers to the CPI in the nth year relative to the previous year = 100; y_n refers to CPI in the nth year relative to the base year 1990 = 100; n = 2000, …,2020. E_a is the value coefficient of ecosystem service function (Yuan/hm^2); l is the type of grain, where the main grain types are wheat, corn, and soybean; s is the number of grain categories; ml is the area of type l grain (hm^2); pl is the yield per unit area of type i grain in Gansu Province (kg/hm^2); ql is the average price of category i grain in Gansu Province (Yuan/kg); M is the total area of s kinds of grain (hm^2); R is the grain yield per unit arable area in Dunhuang (t/hm^2); R_0 is the grain production per unit arable area in Gansu Province (t/hm^2).

Based on the "Ecosystem Service Values per unit area in different Chinese land ecosystems" (Table 1), we assessed the ecosystem service value in Dunhuang from 1990 to 2020. The value of ecosystem services in the study area was calculated by Equations (11) and (12) [47].

$$ESV = \sum_{i=1}^{r} A_i \times VC_i \quad (11)$$

$$VC_i = \sum_{j=1}^{t} EC_j \times E_a \quad (12)$$

where *ESV* is the ecosystem service value (Yuan/year); i is the land use type; *j* is the ecosystem service type; A_i is the area of type *i* (t/hm²); VC_i is the ESV coefficient of the *i*th land use change type; EC_j is the jth ecosystem service value equivalent; *t* is the number of ecosystem service types; E_a is the value coefficient of ecosystem service function (Yuan/hm²).

2.7. Spatial Autocorrelation

Global spatial autocorrelation analysis is mainly used to measure the correlation and degree of correlation between the spatial distribution of a certain property and its neighboring areas, which can be used to visualize the correlation and difference of a certain spatial phenomenon. In this study, the global Moran's I was used for spatial correlation analysis (Eqs 13, 15) [33,48,49].

Local spatial autocorrelation can be used measure the local spatial correlation and spatial dissimilarity between each grid and the surrounding grids. In this study, local Moran's I was chosen for the spatial aggregation or difference analysis of the independent variables (Eqs 13, 14).

$$I = \frac{\sum_{k=1}^{n}\sum_{f=1}^{n} w_{kf}\,(x_k - \bar{x})(x_f - \bar{x})}{S^2(\sum_k \sum_f w_{kf})} \quad (13)$$

$$I_k = \frac{(x_k - \bar{x})\sum_{f=1}^{n}\sum_{f=1}^{n} w_{kf}\,(x_{kf} - \bar{x})}{S^2} \quad (14)$$

$$S^2 = \frac{1}{n}\sum_{i=1}^{n} w_{kf}\,(x_k - \bar{x}) \quad (15)$$

where n is the total number of grid units; x_k is the observed value of certain attribute in the spatial unit k; x_f is the observed value of certain attribute in the spatial unit f; $\bar{x}$ is the mean value of regional variables; S^2 is the mean square deviation; w_{kf} is the spatial weight value, which is expressed by n dimensional matrix w (n×n).

3. Results

3.1. Land Use Change Characteristics of the Dunhuang Oasis

Grassland is the most important vegetation type in Dunhuang Oasis, accounting for 34.31%–51.41% of the total area (Figure 3). The area of grassland first declined and then increased over 30 years, showing a fragile ecological characteristics. From 1990 to 2010, the total area of grassland in the Dunhuang oasis decreased by 61,026 hm², with a reduction rate of 33.27%. In different coverage grasslands, the area of low-cover grassland decreased by 48,237 hm², with a reduction rate of 36%; The area of grassland with moderate-cover grassland showed an increasing trend of 4396.5 hm², with an increase rate of 16%; the area of high-cover grassland decreased by 17,185.05 hm², with a reduction rate of 80%. However, from 2010 to 2020, the grassland area began to increase, and the total area increased by 16,741.98 hm², with an increase rate of 13.68%. The area of low-cover grassland increased by 13,794.93 hm², with an increase rate of 16%; The area of moderate-cover grassland increased by 2364.75 hm², with an increase rate of 7%; The area of high-cover grassland increased by 582 hm², with an increase rate of 14%. The farmland area showed a rapid and continuous upward trend from 1990 to 2010. In 20 years, the area increased by 18001.26 hm², with an area increase rate of 116.08%. However, the farmland area growth was controlled from 2010 to 2020. In 10 years, the farmland area decreased by 4036.41 hm², with a decrease rate of 12.05%. The built-up land has been expanding continuously for 30 years, with an area increase of 8780.94 hm² and an area increase rate of

320.44%. From 1990 to 2010, the shrub forest area increased by 3124.8 hm² in total, but did not change significantly from 2010 to 2020. The water body area decreased by 205.02 hm² from 1990 to 2010, with a decline rate of 46%; From 2010 to 2020, the water-body area increased by 389.79 hm², with an increase rate of 159%. The broadleaf forest land area remains relatively stable on the whole, and the total area accounted for 1.63% –1.8% of the oasis area (Table 2).

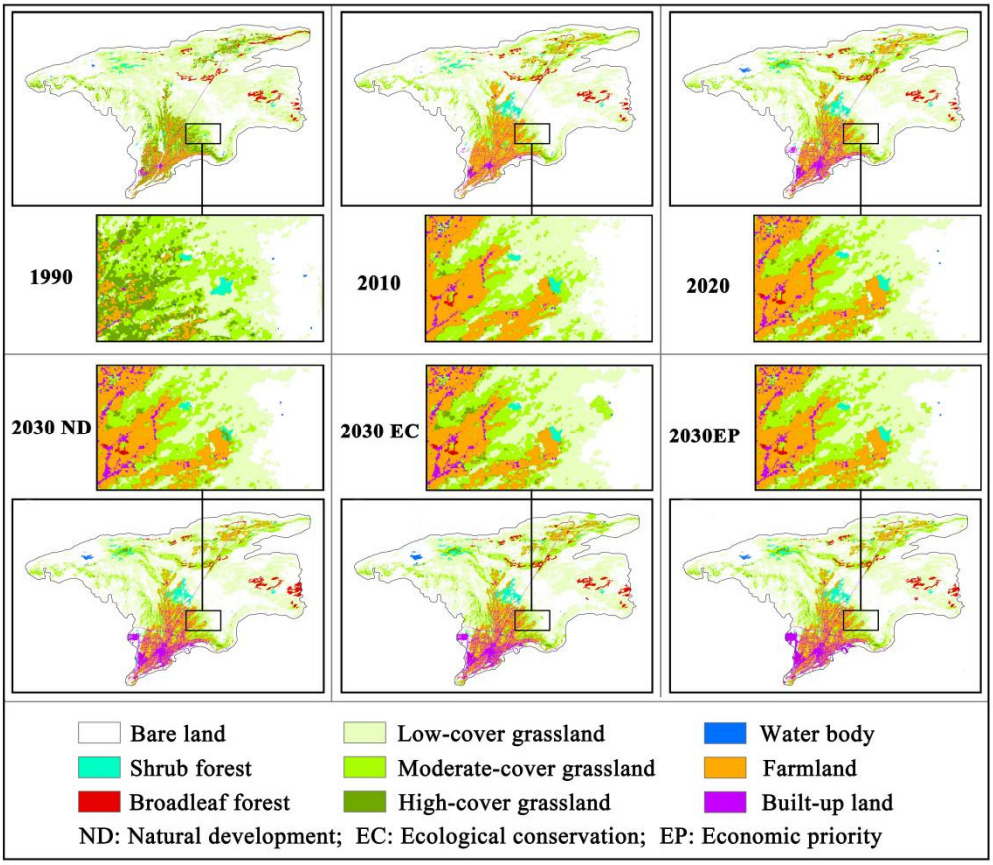

Figure 3. Land use change from 1990 to 2030 under the different scenarios.

Table 2. The Area of different land types in Dunhuang Oasis from 1990–2030 (hm²).

Area	1990	2010	2020	ND	EC	EP
BL	145,891.98	182,675.16	164,711.88	151,849.62	141,154.65	150,111.00
LCG	134,003.07	85,765.41	99,560.34	109,290.69	119,317.95	109,200.78
MCG	28,074.15	32,470.65	34,835.40	37,107.81	35,720.28	36,471.78
HCG	21,355.11	4170.06	4752.36	4344.21	5094.90	4619.34
BF	6402.42	5869.53	5813.19	5916.78	6417.63	5922.63
SF	2387.52	5512.32	5510.52	5258.43	5796.18	5600.07
WB	449.82	244.80	634.59	670.14	936.09	634.14
FL	15,507.54	33,508.80	29,472.39	26,767.98	26,767.98	27,789.39
BU	2740.32	6595.20	11,521.26	15,606.27	15,606.27	16,462.80

Note: BL, bare land; LCG, low-cover grassland; MCG, moderate-cover grassland; HCG, high-cover grassland; SF, shrub forest; BF, broad-leaved forest; FL, farmland; BU, built-up land. ND, natural development; EC, ecological conservation; EP, economic priority.

Using the 2010 and 2020 land use images of the study area as data sources, the AHP-PLUS model was used to simulate the land use pattern of the Dunhuang Oasis in 2030 under three scenarios (ND, EC, and EP). The results show the following:

(1) In the ND scenario, the farmland area has decreased by 2704.41 hm^2, of which 88.53% was converted into built-up land. Grassland is the land type with the largest increase in area, with a total increase of 150,742.71 hm^2. Among them, the low and moderate-cover grassland increased by 9730.35 hm^2 and 2272.41 hm^2 respectively, while the high-cover grassland showed a degradation trend, reducing the area by 408.15 hm^2. The urban area increased by 4085.01 hm^2, an increase of 35%, of which 91% came from bare land and farmland. The area of shrub forest, broadleaf forest and water bodies increased slightly, with an increase rates of 4.57%, 1.78% and 5.60%, respectively (Table 2). (2) In the EC scenario, the grassland area of Dunhuang Oasis has increased by 20985.03 hm^2, with an increase rate of 15.08%. Among them, the area of low-cover, moderate-cover and high-cover grassland showed an increasing trend, with the increase rates of 19.84%, 2.54% and 7.21% respectively. The water body area increased by 301 hm^2, with an increase rate of 47.51%. Compared with 2020, the area of broadleaf forest and shrub forest showed a slow growth trend, with an increase rates of 10.4% and 5.18%, respectively. (3) In the EP scenario, the built-up land mainly expanded to the southwest of the oasis, with an increase of 4941.54 hm^2, or 42.89%. The area of farmland and high coverage grassland decreased by 1683 hm^2 and 133.02 hm^2 respectively. The area of shrub forest and broadleaf forest increased slowly, with an increase ratio of 1.88% and 1.62%. The water body area did not fluctuate significantly (Figure 3).

The three development scenarios focus on different development strategies, and different types of land area change trends are also different. Broadleaf forest, shrub forest, grassland and water bodies have the best protection effect under the ecological protection scenario, and the area increase rate is significantly higher than that under the other scenarios. Under the EC scenario, the grassland area increased by 15.08%, 81% and 88.31% faster than that under the ND scenario and the EP development scenario respectively, and the internal structure of the grassland was significantly improved. The grassland area of all types showed an increasing trend. The area growth rate of forest land, shrub and water bodies were 10.40%, 5.18% and 47.51% respectively, which were also faster than those in the other two scenarios. However the area of high-cover grassland showed a decreasing trend under the ND scenario and the EP development scenarios. In the ND scenarios, the built-up area increased at the fastest rate, increasing by 4941.5 hm^2, 20.97% faster than other scenarios. In the EP scenarios, the reduction of farmland area is the lowest, 37.78% slower than that in the other two scenarios (Table 2).

In terms of spatial distribution, the built-up land areas of the Dunhuang Oasis are mainly concentrated in the southwest, and the farmland is distributed around the city. Broadleaf forest and shrub forest are mainly distributed in the north and east of the oasis, and the water body is mainly concentrated in the northwest. As a whole, the grassland in the Dunhuang Oasis is the most widely distributed, and other land types show a pattern of taking built-up land as the center, farmland, broadleaf forest land (broadleaf forest and shrub forest), and bare land in turn (Figure 3).

3.2. Dunhuang Oasis ESV Change Characteristics

The ESV in 1990, 2010 and 2020 were 9068.15 × 10^6 yuan, 6271.23 × 10^6 yuan and 6916.35 × 10^6 yuan respectively, showing a decreasing and then increasing trend (Figure 4a). Among all land types, grassland had the highest ESV, contributing more than 80% to the total ESV. From 1990 to 2010, the grassland ESV decreased by 3050.16×10^6 yuan, 37.61% less than that in 1990. From 2010 to 2020, the grassland ESV began to recover, increasing by 12.28% compared with that in 2010. In terms of grassland with different coverage, ESV of low-cover and high-cover grassland showed a downward trend from 1900 to 2010, which decreased by 36% and 80.47% respectively compared with 1990. From 2010 to 2020, the growth rate were 16.08% and 13.96% respectively. The ESV of medium coverage grassland increased 432×10^6 yuan in 30 years, with an increase rate of 24.08%. During the past 30 years, the ESV of farmland increased first and then decreased. From 1990 to 2010, the area increased by 149.62×10^6 yuan, 116.08% higher than that in 1990. From 2010

to 2020, it decreased by 33.55×10⁶ yuan, 12.05% compared with that in 2010. The ESV value of the water body showed a downward trend from 1990 to 2010, which was 45.58% lower than that in 1990, but the ESV value of the water body in 2020 was 159.23% higher than that in 2010. The fluctuation of broadleaf forest decreased slowly by 9% from 1990 to 2020; The ESV of shrub forest increased by 130.88% in 2010 compared with 1990, and remained stable in other periods.

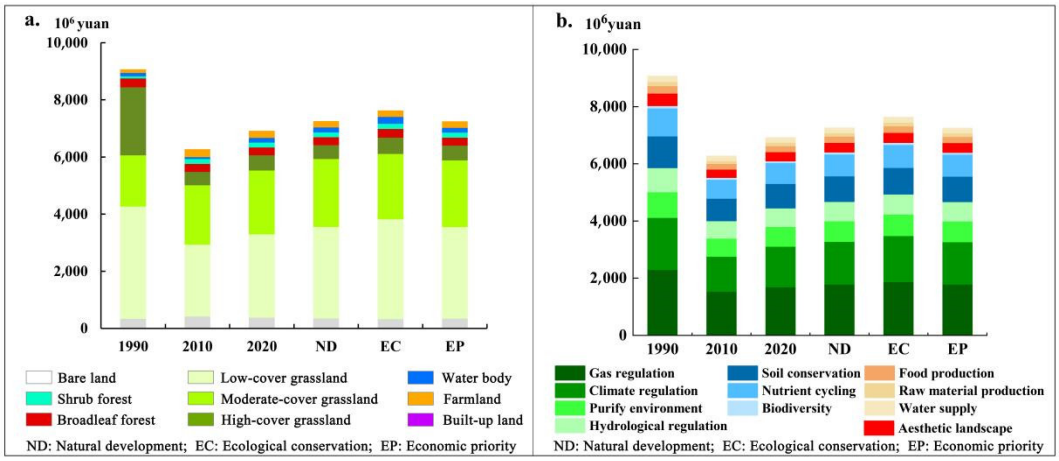

Figure 4. Ecosystem service values (ESV) from 1990 to 2030. (**a**) For the different land use types; (**b**) for the different service types.

In the three scenarios of ND, EC and EP, the predicted values of ESV in the Dunhuang Oasis are 7256.44 × 106 yuan, 7631.07 × 106 yuan and 7249.98 × 10⁶ yuan respectively, an increase of 4.91%, 10.33% and 4.82% compared with 2020 (Figure 5). (1) In the ED scenario, grassland is the land type with the largest increase in ESV, increased by 385.36×10⁶ yuan compared with 2020, of which 66.29% is from bare land, 12.49% is from shrub forest, and 16.36% is from broadleaf forest. However, different coverage grasslands did not show a unified change trend. The ESV of low-cover and moderate-cover grasslands increased by 285.36 × 106 yuan and 145.50 × 106 yuan respectively, while that of high-coverage grassland decreased by 45.52 × 106 yuan. The ESV of farmland decreased by 22.48 × 10⁶ yuan, of which 66.49% was converted to moderate-cover grassland. The ESV of shrub forest, broadleaf forest and water body changed little, increased by 3.4 × 10⁶ yuan, 6.83 × 10⁶ yuan and 9.26 × 10⁶ yuan respectively, with the increase rates of 2%, 2.5% and 5.6% respectively. (2) In the EC scenario, the ESV of grassland increased by 674.34 × 10⁶ yuan, and the area of all types of grassland within the grassland showed an increasing trend. The contributions of low-cover, moderate-cover and high-cover grassland to the total ESV added value of grassland was 85.93%, 8.4% and 5.67% respectively. The ESV of farmland decreased by 22.48 ×10⁶ yuan, and 60.51% of the reduction was converted to moderate-cover grassland and 37.71% to high-cover grassland. The ESV of shrub forest and broadleaf forest increased slightly, with the added value of 9.01 × 10⁶ yuan and 28.76 × 10⁶ yuan, respectively, and the increase rate was 5.18%., and 10.4%. Different from other scenarios, in the ecological protection scenario, the ESV of water body has the largest increase, increasing by 78.5×10⁶ yuan compared with 2020. (3) In the EP development scenario, the ESV of low and moderate-cover grassland increased by 282.75 × 10⁶ yuan and 104.73 × 10⁶ yuan, respectively, with an increase rate of 9.68% and 4.7%, while that of high-cover grassland decreased by 14.84 × 10⁶ yuan, with a decrease rate of 3%. The ESV of farmland decreased by 13.99 × 10⁶ yuan, with a reduction rate of 5.71%. ESV of water body decreased by 0.12 × 10⁶ yuan compared with 2020, with a decrease rate of 0.07%. Compared with 2020, the added value of shrub forest and broadleaf forest is 2.83 × 10⁶ yuan and 5.21 × 10⁶ yuan respectively, with an increase rate of 1.63% and 1.88% respectively.

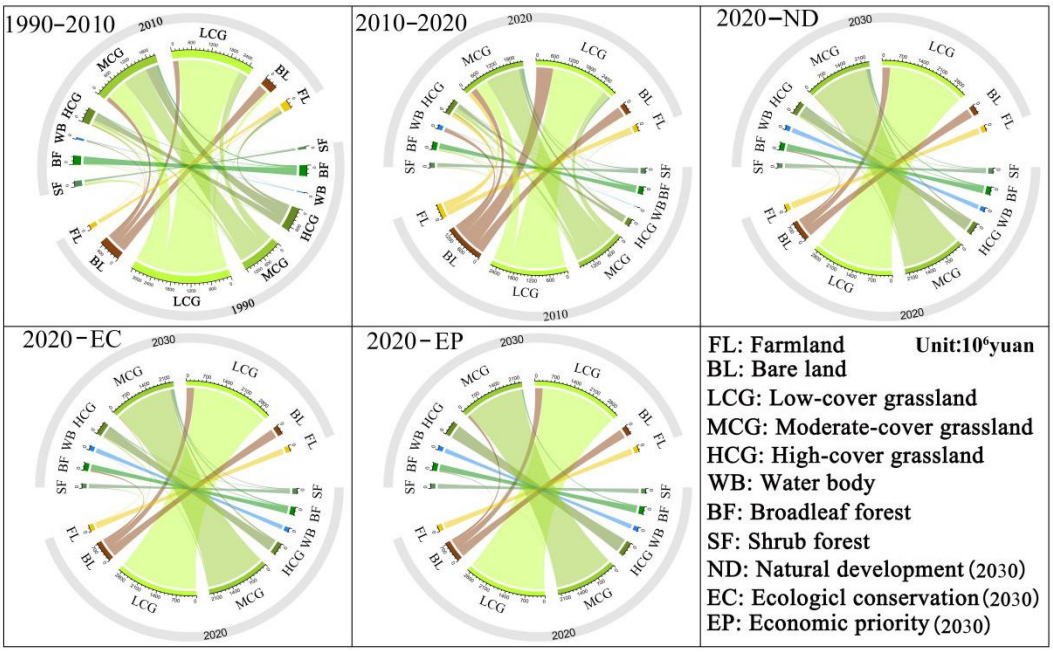

Figure 5. Ecosystem service value (ESV) changes caused by land use change from 1990 to 2030 under the different scenarios.

The predicted results of the three scenarios show that the ESV of grassland, broadleaf forest, shrub forest and water body all show an increasing trend under the EC scenario, and the increase is the highest among the three scenarios. The ESV of agricultural land decreases the least under the EP development scenario, and the ESV of grassland increases the least under this scenario. Under the ND scenario, only the ESV of shrub forest shows a decreasing trend, and the ESV of broadleaf forest increases the least under this scenario (Figure 5).

Figure 4b reflects the pattern of change in the individual ESVs, where each individual ESV service shows a decreasing trend from 1990 to 2010, but an increasing trend after 2010. The degree of contribution of different types of services is in the order of regulation regulating services > supporting services > provisioning services > cultural services. Among the individual services, climate regulation, hydrological regulation, soil conservation and biodiversity contribute more, and in 2020, for example, their percentages were 24.41%, 20.53%, 12.32% and 10.52% respectively, generating an average annual ESV of 4688.98×10^6 yuan. The relationship between the ESV within each individual service under the three scenarios is the same as described above. However, the EC scenario had the largest difference in ESV for regulating services compared to the other 2 scenarios. Provisioning services and cultural services had the smallest differences across all scenarios.

3.3. Spatial Autocorrelation Analysis

3.3.1. Global Spatial Autocorrelation of ESV

Moran scatter plots for the period from 1990 to 2020 and 2030 based on the ND, EC, and EP scenarios were generated. Figure 6 shows that Moran's I was highest in the study area in 1990 and did not fluctuate significantly in the rest of the periods or scenarios, and the values were 0.771, 0.712, 0.714, 0.723, 0.715, and 0.717, respectively. The above values of the Moran's I were all greater than 0.7 and mainly distributed in quadrants one and three, indicating that the distribution pattern of ESV in the study area exhibited obvious clustering and a positive correlation.

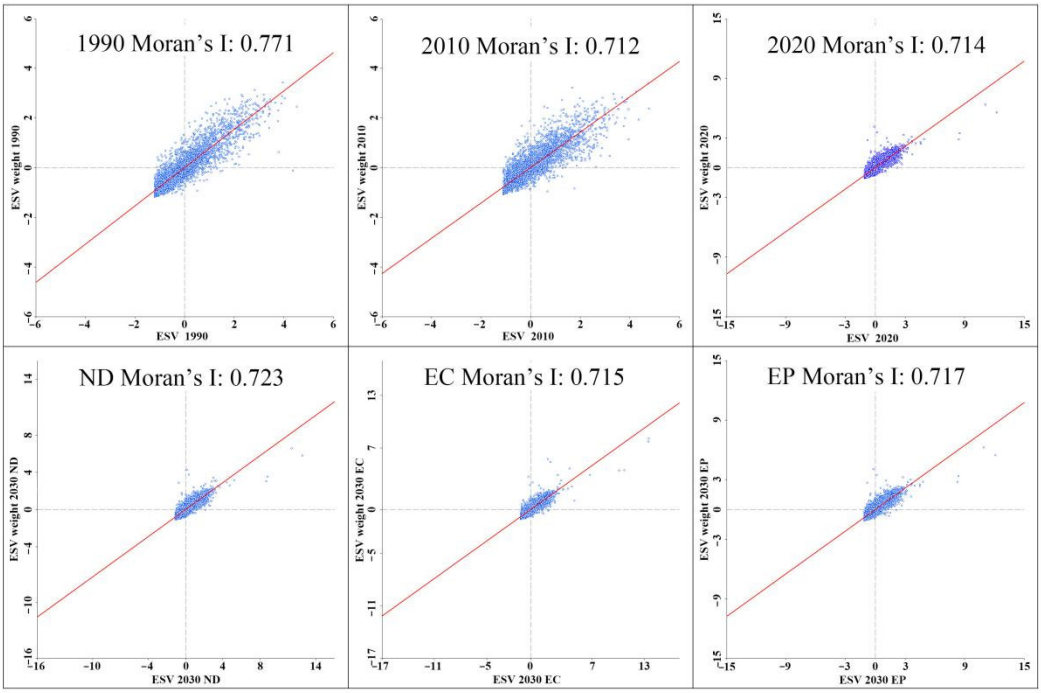

Figure 6. Moran scatter plots of the Ecosystem Service Values in the study area. Note: ND, natural development; EC, ecological conservation; EP, economic priority.

3.3.2. Local Spatial Autocorrelation of ESV

To reveal the local spatial clustering pattern of ESV in the study area, we conducted local spatial autocorrelation analysis based on local indicators of spatial association (LISA) at the 0.001 significance level (Figure 7), and the analysis results classified the autocorrelations of the 1×1 km unit grid in the study area into 4 categories: high-high (HH), low-low (LL), low-high (LH) and high-low (HL). By comparing the land use distribution map and ESV LISA clustering map, we found that HH was mainly found in farmland, moderate-cover, grassland, and woodland, LL was primarily found in bare land, and LH was mainly found in a waterbody and its surrounding areas. HL was mainly found in the transition zone between bare land and grassland.

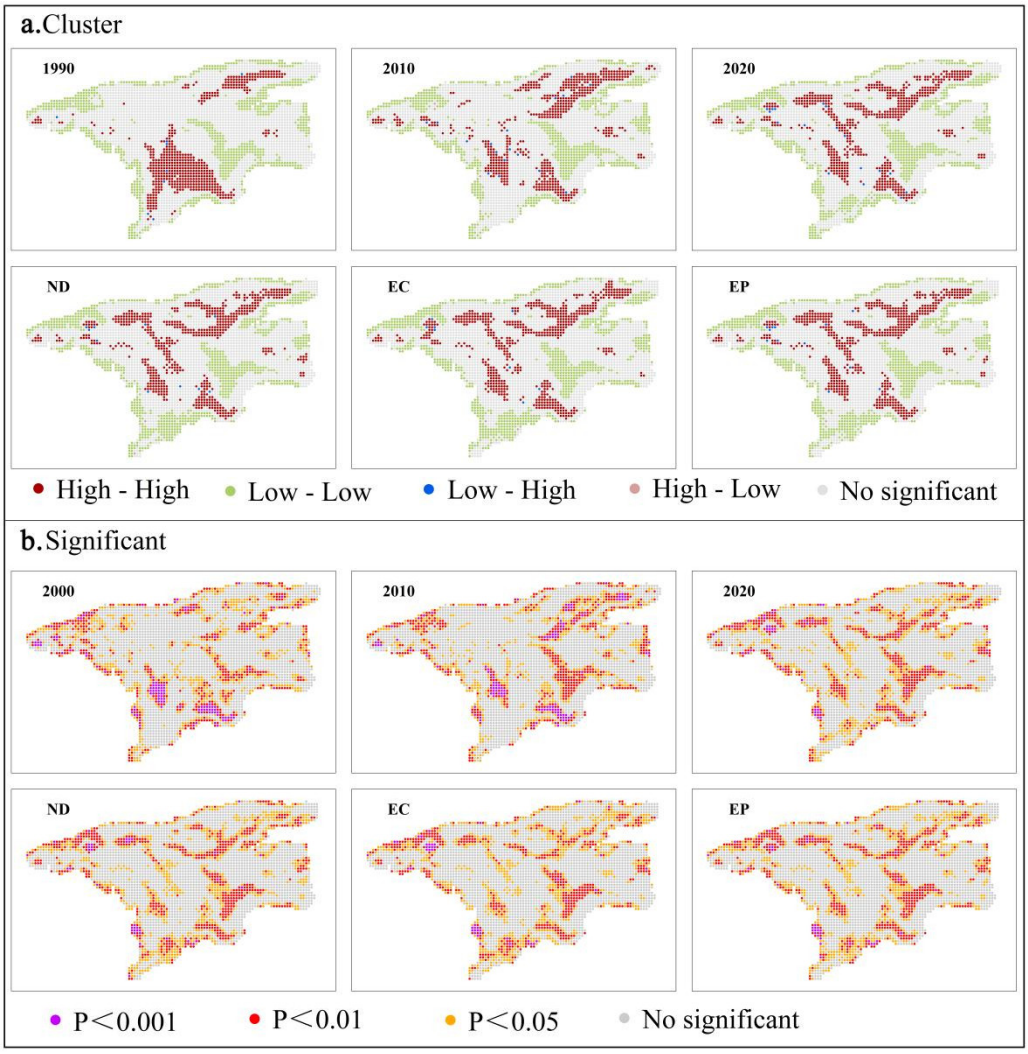

Figure 7. LISA (**a**) cluster and (**b**) significance Map. Note: ND, natural development; EC, ecological conservation; EP, economic priority.

The spatial clustering of ESVs varied considerably between 1990 and 2010. The HH values in 1990 were most concentrated and distributed in the southwest and northeast of the oasis. After 2010, the clustering weakened and expanded to the northwest of the oasis. The clustering relationships of ESV did not change significantly based on the three projection scenarios in 2030. The HH zone was mainly distributed in the northern, central, and southeastern parts of the oasis, exhibiting a patchy pattern, while the LL zone was mainly distributed in the southeastern part and the edge of the oasis.

4. Discussion

4.1. Impact of Human Activities on Land Use Change

The results showed that the bare land area of the Dunhuang Oasis increased by 12.9% during the period from 1990 to 2020, indicating that the region was in a state of ecological degradation. The natural vegetation ecosystem had the largest degraded area of low-coverage grassland, especially before 2010, with degradation accounting for more than one-third of the area. Several studies have found that population growth and economic development in arid regions leads to a decline in the regional groundwater level, which in turn caused extensive vegetation mortality [50,51]. Between 1990 and 2010, the population and GDP of the Dunhuang Oasis increased by 4.2 and 1.71 times (Figure 8a), respectively, and water for production and domestic use compressed the ecological water consumption by

the vegetation [52,53]. After 2010, the Dunhuang government strictly controlled groundwater mining, and low-cover grasslands recovered to some extent [54]. Although the degraded area of high-cover grassland was lower than that of low-cover grassland, its degradation percentage was 77.75%, the largest among all land use types. The degradation of high-coverage grassland mainly occurred during the period from 1990 to 2010, when residents were forced to reclaim farmland on a large scale due to economic pressure. High-cover grassland was distributed between settlements and farmland, with the advantages of abundant water, convenient transportation, and proximity to settlements, making it an ideal target for reclamation, thus, the area declined significantly [55]. After the 21st century, the government restricted farmland reclamation, and the degradation trend of high-cover grasslands was curbed, but no significant recovery has occurred. Broad-leaved forest has been in a state of continuous degradation for the past 30 years, mainly in the northeastern part of the oasis, where the primary species of the broad-leaved forest is the *Populus euphratica* which grows near the river. However, in the late 1970s, the Shule River in the northern part of the oasis dried up due to the construction of reservoirs upstream, resulting in extensive degradation of *Populus euphratica* around the river [56]. During 1990–2020, the built-up land area of the Dunhuang oasis continued to expand, which was consistent with Zhang's research in the Hexi Corridor [57]. Unlike its predecessors, Dunhuang's built-up land expansion in the last decade did not cause ecological degradation, mainly due to the implementation of a tourism-based industrial development route in Dunhuang which strengthened the government's focus on the environment and thus contributed to the conservation of the oasis ecosystem (Figure 8b). Overall, the Dunhuang oasis was in a degraded state during the period from 1990 to 2010, and the ecological situation was mitigated after 2010 with the introduction of a series of environmental policies.

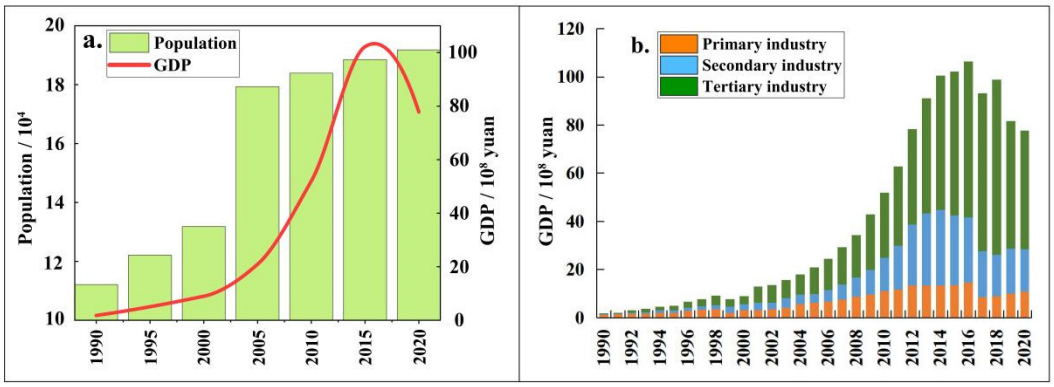

Figure 8. Social economic dynamics of Dunhuang Oasis, changes in population and GDP of Dunhuang from 1990 to 2020 (**a**), changes in economic structure of Dunhuang from 1990 to 2020 (**b**).

4.2. Effect of Land Use Change on ESV

During the period from 1990 to 2020, the Dunhuang Oasis ESV experienced a decrease followed by an increase, a trend consistent with that found by most studies in China [16,21,58]. This was mainly due to conditions from 1990 to 2010 when China entered a period of rapid development, and built-up land and farmland occupied a large number of forests, grassland, and waterbodies during the period, resulting in a significant decrease in ESV. After 2010, the government paid more attention to ecological conservation, and the ecological water supplement project—"Haerteng River-to-Dang River water diversion" was conducted in 2015. The area of the waterbody in 2020 increased to 2.59 times that in 2010, and the ESV began to recover. The contribution of grasslands to the change in ESV was the greatest in the ESV degradation period (1990–2010) and the ESV growth period (2010–2020). This was consistent with the work of Rao et al. [36] who found that, in the arid area, grassland had the highest ESV among all land use types.

Considering the wide distribution of grasslands in the arid area, it is necessary to explore their influence on ESV more thoroughly. Through the analysis of different cover grasslands, we found that high-cover grassland contributed the most during the declining ESV period but contributed the least during the rising ESV period, mainly because of the frequent farmland reclamation activities in the Dunhuang Oasis during the declining period when the high-cover grasslands closer to settlements were reclaimed as farmland. The high-cover grasslands farther away from settlements did not attract the interest of farmers, but their plant species are mainly Phragmites australis, Tamarix chinensis, etc. which are very sensitive to groundwater changes. The decrease in groundwater level due to agricultural irrigation, the degradation of plant communities and their replacement by more drought-tolerant plant communities, or the change in land use type from high-cover grassland to low-cover grassland or bare ground due to the increase in soil salinity led to a decrease in ESV [56,59]. During the period of rising ESV, the increase in ESV of high-cover grassland was lower than that of moderate- and low-cover grassland because high-cover grassland requires high soil and moisture conditions and recovers slowly, thus resulting in the lowest ESV increase. Overall, during the period of ESV decline, high-cover grassland was affected by both direct (farmland reclamation) and indirect (groundwater level decline) human activities, resulting in a significant decrease in ESV; during the period of ESV increase, high-cover grasslands had a higher demand for water, resulting in a slow increase in ESV [60].

Spatial analysis showed that the areas with higher ESV were concentrated in the northern part of the oasis, and the lower areas occurred in the northeast and southwest of the oasis. The main reason was that the northern part of the oasis was mainly dominated by broad-leaved forests and grasslands, while the northeast and central parts were mainly dominated by farmland and construction land. The Moran index values of ESV were greater than 0.7 in all periods and positively correlated, which is a clear indication that ESV was regulated by land use [61]. After 1990, the expansion of farmland in Dunhuang Oasis, replacement of high-cover grassland, built-up land expansion, and road construction, fragmented the original natural vegetation communities, resulting in the distribution of HH areas in the central part of the study area becoming less aggregated. The area of HH in the northeast of the oasis expanded from 2010 to 2020, which was mainly because the employment direction of residents was transferred from the primary industry to the secondary and tertiary industries [13]. The farmland in the north of the oasis was abandoned in a large area and then converted into grasslands and shrub forests, thus, the ESV aggregation in the region was enhanced.

4.3. Land Use Change and ESV Changes in the Future

The prediction results showed that, based on the different scenarios, the order of the ESV size ranking was as follows: EC > ND > EP. This indicated that the implementation of different land management policies contributed to ecological restoration [62,63]. In the EC scenario, the increased area of low-coverage grassland was significantly larger than that in the others scenarios, and the increased area was mainly distributed along the Shule River, which benefited from the implementation of the ecological water supplement project. Compared to ND, the large increase in farmland and built-up land area in the EP scenario led to a decrease in the ESV of the Dunhuang Oasis (except for farmland), with a decrease of nearly 12.67×10^6 yuan in high-cover grassland. These results indicated that this scenario did not support the sustainable development of the Dunhuang Oasis and that the government should limit built-up land and farmland expansion in future decisions. The EC scenario can be used as a reference to protect forests and waterbodies, restrict production and domestic water consumption and increase the proportion of ecological water consumption.

4.4. Limitations and Future Work of the Study

Ecosystems in arid area are fragile and need a reasonable assessment method to guide ecological conservation and restoration efforts. The assessment of oasis ESVs can meet this need, but there are some problems. (1) The scale of oasis cities is small, so we must use medium/high resolution satellite images for land use interpretation, but there are few publicly available medium/high resolution meteorological raster datasets. In this study, we had used station data to interpolate historical year meteorological data in a pre-experiment, but the meteorological stations around the study area were 200 km away and unevenly distributed (Kumutag Desert in the west of the Dunhuang Oasis and Aljinshan Glacier in the south), and the final data did not meet the criteria for use. The above factors made it difficult to conduct meteorological driver analysis, and in future studies we expect to deploy more stations to meet the conditions for analysis. (2) The slow economic development of Northwest China and the lack of historical economic statistics (grain prices, etc.) for many county-level cities made it difficult to avoid ESV assessment errors, although we balanced these using the 1990–2020 China Price Inflation Index, the ratio of grain production in Gansu Province to Dunhuang City. In future research, more economic knowledge needs to be incorporated to improve the accuracy of ESV assessment.

5. Conclusions

In this study, we interpreted the land use type of Dunhuang Oasis in a hyperarid area from 1990 to 2020. Then, we combined it with socio-economic statistics; the ESV was evaluated by the benefit transfer method, and finally, the AHP-PLUS model was used to predict the changes of land use type and ESV under three scenarios in 2030. The results showed the following: (1) In the past 30 years, the built-up land area of Dunhuang Oasis has rapidly increased, the area of farmland reached the maximum in 2010, and the grassland has been seriously degraded, amounting to 44,285.76 hm^2. (2) Between 1990–2010, farmland reclamation led to a large decline in high-cover grassland. Built-up land expansion, and population growth caused by the decline in groundwater resulted in extensive degradation of low-coverage grassland. After 2010, the implementation of ecological diversion restricted groundwater mining and other policies and promoted the recovery of natural vegetation in Dunhuang Oasis. (3) ESV first decreased and then increased, with a cumulative loss of 2151.4 $\times 10^6$ yuan over the last 30 years, grassland contributed the most to ESV and had a large influence on its trend. (4) The ESV for the year 2030 under different scenarios was ranked as follows: ecological conservation > natural development > economic priority. In the ecological conservation scenario, 10532.34 hm^2 of vegetation, 301.95 hm^2 of the waterbody, and 381.1 $\times 10^6$ yuan of ESV were added compared to those under the economic priority scenario. Based on the above results, we suggest that the government refer to the ecological conservation scenario, limit the expansion of built up land and farmland, increase the proportion of ecological water consumption, promote the restoration of water bodies and grasslands, and improve the ESV of Dunhuang Oasis; In addition, our research shows that the area of grassland is the dominant factor of ESV in Dunhuang Oasis. Therefore, according to the area and coverage of grassland, it is very important to develop a theoretical framework for ESV assessment in arid areas to improve the accuracy of oasis ESV assessment. This study not only estimates and forecasts the ESV of Dunhuang Oasis in a more detailed way, but also focuses on the grassland evaluation model, which is also of good reference significance for the future oasis ESV evaluation.

Author Contributions: Writing original draft, F.Y. and Q.Y.; visualization, F.Y. and Q.Y.; conceptualization, F.Y.; methodology, F.Y. and Q.Y.; data curation, B.Y.; investigation, Y.L., L.C., Q.L. and Z.W.; funding acquisition, Z.W.; writing—review& editing, Y.L., Q.L. and L.C. All authors read and contributed to the manuscript. F.Y. and Q.Y. contributed equally to the study and are first co-authors. All authors have read and agreed to the published version of the manuscript.

Funding: This work is supported by the Central Non-profit Research Institution of Chinese Academy of Forestry (CAFYBB2020ZE005, CAFYBB2020GD001), the Major Horizontal Project of the

analysis and research on ecological background check and eco-hydrological monitoring of Dunhuang West Lake National Nature Reserve and its surrounding areas (JQDHXHSTSW/JC-2018.06), Special monitoring of desert ecosystem ecological function value assessment (2020062033), and Technology for improving desert ecosystem service function in Xinjiang (2021B03002-3).

Acknowledgments: We appreciate the critical and constructive comments and suggestion from the reviewers that helped to improve the quality of this manuscript. We also would like to offer our sincere thanks to those who participated in the data processing and provided constructive comments for this study.

Conflicts of Interest: The authors declare no conflict of interest.

Appendix A

Table A1. Confusion matrix of land use mapping in Dunhuang oasis in 1990.

Classification data	Standard data									Row Statistics	Users accuracy
	BL	LCG	MCG	HCG	SF	BF	WB	FL	BU		
BL	363	42	2	0	0	0	0	2	1	410	0.89
LCG	24	341	7	1	0	0	0	0	0	373	0.91
MCG	2	7	54	1	0	0	0	3	0	68	0.79
HCG	0	2	5	56	1	0	0	5	0	69	0.81
SF	0	1	2	1	14	1	0	1	0	20	0.70
BF	0	0	0	0	0	3	0	0	0	3	1.00
WB	0	0	0	0	0	0	2	0	0	2	1.00
FL	0	0	2	2	0	0	0	41	0	45	0.91
BU	1	1	0	0	0	0	0	1	7	10	0.70
Column Statistics	390	394	72	61	15	4	2	53	8		
Produce accuracy	0.93	0.87	0.75	0.92	0.93	0.75	1.00	0.77	0.88		
Overall accuracy	0.88			Kappa coefficient 0.83							

Note: BL, bare land; LCG, low-cover grassland; MCG, moderate-cover grassland; HCG, high-cover grassland; SF, shrub forest; BF, broad-leaved forest; FL, farmland; BU, built-up land. ND, natural development; EC, ecological conservation; EP, economic priority.

Table A2. Confusion matrix of land use mapping in Dunhuang oasis in 2010.

Classification data	Standard data									Row Statistics	Users accuracy
	BL	LCG	MCG	HCG	SF	BF	WB	FL	BU		
BL	436	51	3	0	1	1	0	5	6	503	0.87
LCG	18	201	6	0	0	2	0	0	0	227	0.89
MCG	2	5	78	0	0	1	0	4	0	90	0.87
HCG	0	0	2	7	0	0	0	1	0	10	0.70
SF	0	2	0	0	12	1	0	0	0	15	0.80
BF	0	0	2	0	2	21	0	0	0	25	0.84
WB	1	0	0	0	0	0	4	0	0	5	0.80
FL	1	0	3	3	1	0	0	83	1	94	0.88

BU	3	2	0	0	0	0	0	0	26	31	0.84
Column Statistics	461	261	94	10	16	26	4	93	33		
Produce accuracy	0.95	0.77	0.83	0.70	0.75	0.81	1	0.89	0.79		
Overall accuracy	0.87			Kappa coefficient 0.81							

Note: BL, bare land; LCG, low-cover grassland; MCG, moderate-cover grassland; HCG, high-cover grassland; SF, shrub forest; BF, broad-leaved forest; FL, farmland; BU, built-up land. ND, natural development; EC, ecological conservation; EP, economic priority.

Table A3. Confusion matrix of land use mapping in Dunhuang oasis in 2020.

Classifica-tion data	**Standard data**									**Row Statistics**	**Users accuracy**
	BL	**LCG**	**MCG**	**HCG**	**SF**	**BF**	**WB**	**FL**	**BU**		
BL	413	21	5	0	2	1	0	2	1	445	0.93
LCG	17	261	10	0	0	3	0	0	0	291	0.90
MCG	3	7	86	1	0	1	0	3	0	101	0.85
HCG	0	0	1	7	0	0	0	2	0	10	0.70
SF	1	4	1	0	9	0	0	0	0	15	0.60
BF	0	1	1	0	1	12	0	0	0	15	0.80
WB	1	0	0	0	0	0	2	0	0	3	0.67
FL	3	1	1	2	0	0	0	80	1	88	0.91
BU	2	1	0	0	0	0	0	1	28	32	0.88
Column Statistics	440	296	105	10	12	17	2	88	30		
Produce accuracy	0.94	0.88	0.82	0.70	0.75	0.71	1.00	0.91	0.93		
Overall accuracy	0.90			Kappa coefficient 0.85							

Note: BL, bare land; LCG, low-cover grassland; MCG, moderate-cover grassland; HCG, high-cover grassland; SF, shrub forest; BF, broad-leaved forest; FL, farmland; BU, built-up land. ND, natural development; EC, ecological conservation; EP, economic priority.

Table A4. The importance of factors in AHP.

Intensity of importance on an absolute scale	**Explanation**
1	Indicates that two factors are of equal importance compared to each other
3	Indicates that the former is slightly more important than the latter when compared to the two factors
5	Indicates that the former is significantly more important than the latter when compared to the two factors

7	Indicates that the former is more strongly important than the latter when compared to the two factors
9	Indicates that the former is more extremely important than the latter when compared to the two factors
2、4、6、8	Denotes the middle value of the above adjacent judgement
Countdown	If the ratio of the importance of factor i to factor j is a_{ij}, then the ratio of the importance of factor j to factor i is $a_{ji}=1/a_{ij}$

Table A5. RI of low order judgment matrix.

m	1	2	3	4	5	7	8	9	10
RI	0	0	0.57	0.9	1.12	1.32	1.41	1.45	1.49

Table A6. Ecosystem service value changes from 1990 to 2010 (106 yuan).

2010 / 1990	BL	LCG	MCG	HCG	BF	SF	WB	FL
BL	307.37	107.07	1.20	0.24	0.01	0.02	0.51	0.03
LCG	172.41	2043.58	279.96	15.36	1.87	0.95	0.81	0.36
MCG	134.72	695.90	802.40	368.63	58.05	3.08	5.90	8.81
HCG	32.38	69.74	96.96	229.84	22.27	1.53	1.88	10.05
BF	1.96	15.06	8.18	7.51	244.64	0.01	0.03	1.72
SF	15.64	76.54	8.26	3.95	0	68.61	0.05	0.17
WB	29.20	8.25	2.81	3.73	2.41	0	16.33	1.01
FL	10.31	22.03	31.21	96.23	0.58	0.90	0.14	116.19

Note: BL, bare land; LCG, low-cover grassland; MCG, moderate-cover grassland; HCG, high-cover grassland; SF, shrub forest; BF, broad-leaved forest; FL, farmland.

Table A7. Ecosystem service value changes from 2010 to 2020 (106 yuan).

2020 / 2010	BL	LCG	MCG	HCG	BF	SF	WB	FL
BL	356.44	17.43	0.76	0.03	0.13	0.20	0.25	0.12
LCG	597.52	2011.87	255.06	3.10	24.15	18.39	0.78	7.39
MCG	212.51	461.36	1220.71	104.03	44.23	30.68	2.00	149.53
HCG	33.06	67.89	147.27	136.91	11.00	10.20	0.66	121.88
BF	10.22	38.94	26.88	2.31	187.44	0.16	0.11	7.96
SF	7.88	18.96	11.96	1.54	0.60	129.18	0.03	3.13
WB	134.38	4.78	9.40	3.12	0	0	12.75	0.35
FL	1.69	1.17	13.55	7.58	1.31	0.87	0.07	216.76

Note: BL, bare land; LCG, low-cover grassland; MCG, moderate-cover grassland; HCG, high-cover grassland; SF, shrub forest; BF, broad-leaved forest; FL, farmland.

Table A8. Ecosystem service value changes from 2020 to 2030 ND (106 yuan).

ND / 2020	BL	LCG	MCG	HCG	BF	SF	WB	FL
BL	345.49	0	0	0	0.28	0.45	0	0
LCG	285.17	2920.06	0	0	0	0	0	0.22
MCG	17.75	0	2187.88	70.94	49.55	34.79	0	15.02
HCG	3.29	0	47.68	377.42	26.04	22.91	0	7.20
BF	61.47	0	1.37	0.23	218.35	0.00	0	0.05
SF	16.00	0	0.81	4.57	0.48	143.95	0	0.08
WB	9.23	0	0	0	0	0	165.22	0.02
FL	0	0	0	0	0	0	0	222.49

Note: BL, bare land; LCG, low-cover grassland; MCG, moderate-cover grassland; HCG, high-cover grassland; SF, shrub forest; BF, broad-leaved forest; FL, farmland. ND, natural development.

Table A9. Ecosystem service value changes from 2020 to 2030 EC (106 yuan).

EC / 2020	BL	LCG	MCG	HCG	BF	SF	WB	FL
BL	321.46	0.37	0.01	0	0	0	0	0
LCG	548.44	2899.75	50.51	0.64	0	0	0	0.20
MCG	177.28	30.48	2007.18	57.73	0	0	0	14.41
HCG	0.69	0.42	146.42	411.76	0	0	0	8.97
BF	21.53	0.61	6.06	0.50	276.53	0	0	0.05
SF	5.13	0.11	3.33	0.34	0	173.84	0	0.10
WB	75.05	0.54	2.16	0.68	0	0	165.22	0.07
FL	0	0	0	0	0	0	0	222.49

Note: BL, bare land; LCG, low-cover grassland; MCG, moderate-cover grassland; HCG, high-cover grassland; SF, shrub forest; BF, broad-leaved forest; FL, farmland. EC, ecological conservation.

Table A10. Ecosystem service value changes from 2020 to 2030 EP (106 yuan).

EP / 2020	BL	LCG	MCG	HCG	BF	SF	WB	FL
BL	342.09	0	0.01	0	0.16	0	0	0
LCG	282.56	2920.06	0	0.19	0	0	0	0
MCG	96.39	0	2191	7.06	40.72	0	0.02	0
HCG	0	0	0	515.22	0	0	0	0
BF	27.09	0	11.82	0.07	242.77	0	0	0
SF	1.79	0	0.87	0.03	0.13	173.84	0	0
WB	0	0	0	0	0	0	165.10	0
FL	0	0	0	0	0	0	0	230.98

Note: BL, bare land; LCG, low-cover grassland; MCG, moderate-cover grassland; HCG, high-cover grassland; SF, shrub forest; BF, broad-leaved forest; FL, farmland. EP, economic priority.

Reference

1. Rey Benayas, J.M.; Newton, A.C.; Diaz, A.; Bullock, J.M. Enhancement of biodiversity and ecosystem services by ecological restoration: A meta-analysis. *Science* **2009**, *325*, 1121–1124. https://doi.org/10.1126/science.1172460.
2. Ouyang, Z.; Zheng, H.; Xiao, Y.; Polasky, S.; Liu, J.; Xu, W.; Wang, Q.; Zhang, L.; Xiao, Y.; Rao, E.; et al. Improvements in ecosystem services from investments in natural capital. *Science* **2016**, *352*, 1455–1459. https://doi.org/10.1126/science.aaf2295.
3. Braat, L.C.; de Groot, R. The ecosystem services agenda: Bridging the worlds of natural science and economics, conservation and development, and public and private policy. *Ecosyst. Serv.* **2012**, *1*, 4–15. https://doi.org/10.1016/j.ecoser.2012.07.011.
4. Costanza, R.; de Groot, R.; Braat, L.; Kubiszewski, I.; Fioramonti, L.; Sutton, P.; Farber, S.; Grasso, M. Twenty years of ecosystem services: How far have we come and how far do we still need to go? *Ecosyst. Serv.* **2017**, *28*, 1–16. https://doi.org/10.1016/j.ecoser.2017.09.008.
5. Wu, C.; Chen, B.; Huang, X.; Wei, Y.H.D. Effect of land-use change and optimization on the ecosystem service values of Jiangsu province, China. *Ecol. Indic.* **2020**, *117*, 106507. https://doi.org/10.1016/j.ecolind.2020.106507.
6. Hasan, S.S.; Zhen, L.; Miah, M.G.; Ahamed, T.; Samie, A. Impact of land use change on ecosystem services: A review. *Environ. Dev.* **2020**, *34*, 100527. https://doi.org/10.1016/j.envdev.2020.100527.
7. Song, F.; Su, F.; Mi, C.; Sun, D. Analysis of driving forces on wetland ecosystem services value change: A case in northeast China. *Sci. Total Environ.* **2021**, *751*, 141778. https://doi.org/10.1016/j.scitotenv.2020.141778.
8. SMITH, E. Extinction—The causes and consequences of the disappearance of species -ehrlich,p, ehrlich,a. *South Calif. Law Rev.* **1982**, *55*, 769–783.
9. EHRLICH, P.; MOONEU, H. Extinction, substitution, and ecosystem services. *Bioscience* **1983**, *33*, 248–254. https://doi.org/10.2307/1309037.
10. DEGROOT, R. Environmental functions as a unifying concept for ecology and economics. *Environmentalist* **1987**, *7*, 105–109. https://doi.org/10.1007/BF02240292.
11. KELLERT, S. Assessing wildlife and environmental values in cost-benefit-analysis. *J. Environ. Manag.* **1984**, *18*, 355–363.
12. Costanza, R.; d'Arge, R.; de Groot, R.; Farber, S.; Grasso, M.; Hannon, B.; Limburg, K.; Naeem, S.; O'Neill, R.V.; Paruelo, J.; et al. The value of the world's ecosystem services and natural capital (reprinted from nature, vol 387, pg 253, 1997). *Ecol. Econ.* **1998**, *25*, 3–15. https://doi.org/10.1016/S0921-8009(98)00020-2.
13. Jiang, C.; Wang, F.; Zhang, H.; Dong, X. Quantifying changes in multiple ecosystem services during 2000–2012 on the loess plateau, china, as a result of climate variability and ecological restoration. *Ecol. Eng.* **2016**, *97*, 258–271. https://doi.org/10.1016/j.ecoleng.2016.10.030.
14. Wang, Y.; Pan, J. Building ecological security patterns based on ecosystem services value reconstruction in an arid inland basin: A case study in ganzhou district, NW China. *J. Clean. Prod.* **2019**, *241*, 118337. https://doi.org/10.1016/j.jclepro.2019.118337.
15. Xiao, R.; Lin, M.; Fei, X.; Li, Y.; Zhang, Z.; Meng, Q. Exploring the interactive coercing relationship between urbanization and ecosystem service value in the shanghai-hangzhou bay metropolitan region. *J. Clean. Prod.* **2020**, *253*, 119803. https://doi.org/10.1016/j.jclepro.2019.119803.
16. Pan, N.; Guan, Q.; Wang, Q.; Sun, Y.; Li, H.; Ma, Y. Spatial differentiation and driving mechanisms in ecosystem service value of arid region:a case study in the middle and lower reaches of shule river basin, NW China. *J. Clean. Prod.* **2021**, *319*, 128718. https://doi.org/10.1016/j.jclepro.2021.128718.
17. Xie, G.D.; Zhen, L.; Lu, C.X.; Cao, S.Y.; Xiao, Y. Supply, consumption and valuation of ecosystem services in China. *Resour. Sci.* **2008**, *38*, 1152–1161. https://doi.org/10.3321/j.issn:1007-7588.2008.01.014.
18. Xie, G.D.; Zhen, L.; Lu, C.X.; Xiao, Y.; Chen, C. Expert knowledge based valuation method of ecosystem services in China. *J. Nat. Resour.* **2009**, *5*, 911–919. https://doi.org/10.3321/j.issn:1000-3037.2008.05.019.
19. Xie, G.D.; Zhang, C.X.; Zhang, L.M.; Chen, W.H.; Li, S.M. Improvement of the evaluation method for ecosystem service value based on per unit area. *J. Nat. Resour.* **2015**, *30*, 1243–1254. https://doi.org/10.11849/zrzyxb.2015.08.001.
20. Xie, G.; Zhang, C.; Zhen, L.; Zhang, L. Dynamic changes in the value of china's ecosystem services. *Ecosyst. Serv.* **2017**, *26*, 146–154. https://doi.org/10.1016/j.ecoser.2017.06.010.
21. Xiao, Y.; Huang, M.; Xie, G.; Zhen, L. Evaluating the impacts of land use change on ecosystem service values under multiple scenarios in the hunshandake region of China. *Sci. Total Environ.* **2022**, *850*, 158067. https://doi.org/10.1016/j.scitotenv.2022.158067.
22. Shuangao, W.; Padmanaban, R.; Mbanze, A.A.; Silva, J.M.N.; Shamsudeen, M.; Cabral, P.; Campos, F.S. Using satellite image fusion to evaluate the impact of land use changes on ecosystem services and their economic values. *Remote Sens.* **2021**, *13*, 851. https://doi.org/10.3390/rs13050851.
23. Wang, X.; Yan, F.; Zeng, Y.; Chen, M.; Su, F.; Cui, Y. Changes in ecosystems and ecosystem services in the guangdong-hong kong-macao greater bay area since the reform and opening up in China. *Remote Sens.* **2021**, *13*, 1611. https://doi.org/10.3390/rs13091611.

24. Millennium Ecosystem Assessment *Ecosystems and Human Well-Being*; Island Press: Washington, D.C., United States of America, 2005.
25. Long, X.; Lin, H.; An, X.; Chen, S.; Qi, S.; Zhang, M. Evaluation and analysis of ecosystem service value based on land use/cover change in dongting lake wetland. *Ecol. Indic.* **2022**, *136*, 108619. https://doi.org/10.1016/j.ecolind.2022.108619.
26. Chen, Z.; Huang, M.; Zhu, D.; Altan, O. Integrating remote sensing and a markov-flus model to simulate future land use changes in Hokkaido, Japan. *Remote Sens.* **2021**, *13*, 2621. https://doi.org/10.3390/rs13132621.
27. Wang, X.; Yan, F.; Su, F. Impacts of urbanization on the ecosystem services in the guangdong-hong kong-macao greater bay area, China. *Remote Sens.* **2020**, *12*, 3269. https://doi.org/10.3390/rs12193269.
28. Dai, X.; Johnson, B.A.; Luo, P.; Yang, K.; Dong, L.; Wang, Q.; Liu, C.; Li, N.; Lu, H.; Ma, L.; et al. Estimation of urban ecosystem services value: A case study of chengdu, southwestern China. *Remote Sens.* **2021**, *13*, 207. https://doi.org/10.3390/rs13020207.
29. Maimaiti, B.; Chen, S.; Kasimu, A.; Mamat, A.; Aierken, N.; Chen, Q. Coupling and coordination relationships between urban expansion and ecosystem service value in kashgar city. *Remote Sens.* **2022**, *14*, 2557. https://doi.org/10.3390/rs14112557.
30. Shi, L.; Halik, U.; Mamat, Z.; Aishan, T.; Abliz, A.; Welp, M. Spatiotemporal investigation of the interactive coercing relationship between urbanization and ecosystem services in arid northwestern China. *Land Degrad. Dev.* **2021**, *32*, 4105–4120. https://doi.org/10.1002/ldr.3946.
31. Maimaiti, B.; Chen, S.; Kasimu, A.; Simayi, Z.; Aierken, N. Urban spatial expansion and its impacts on ecosystem service value of typical oasis cities around tarim basin, northwest China. *Int. J. Appl. Earth Obs. Geoinformation.* **2021**, *104*, 102554. https://doi.org/10.1016/j.jag.2021.102554.
32. UNCCD. *Reaping the Rewards: Financing Land Degradation Neutrality; United Nations Convention to Combat Desertification*; *United Nations Convention to Combat Desertification.* Bonn, Germany, **2015.**
33. Zhang, F.; Yushanjiang, A.; Jing, Y. Assessing and predicting changes of the ecosystem service values based on land use/cover change in ebinur lake wetland national nature reserve, Xinjiang, China. *Sci. Total Environ.* **2019**, *656*, 1133–1144. https://doi.org/10.1016/j.scitotenv.2018.11.444.
34. Tan, Z.; Guan, Q.; Lin, J.; Yang, L.; Luo, H.; Ma, Y.; Tian, J.; Wang, Q.; Wang, N. The response and simulation of ecosystem services value to land use/land cover in an oasis, northwest China. *Ecol. Indic.* **2020**, *118*, 106711. https://doi.org/10.1016/j.ecolind.2020.106711.
35. Fensholt, R.; Langanke, T.; Rasmussen, K.; Reenberg, A.; Prince, S.D.; Tucker, C.; Scholes, R.J.; Le, Q.B.; Bondeau, A.; Eastman, R.; et al. Greenness in semi-arid areas across the globe 1981–2007—an earth observing satellite based analysis of trends and drivers.. *Remote Sens. Environ.* **2012**, *121*, 144–158. https://doi.org/10.1016/j.rse.2012.01.017.
36. Rao, Y.; Zhou, M.; Ou, G.; Dai, D.; Zhang, L.; Zhang, Z.; Nie, X.; Yang, C. Integrating ecosystem services value for sustainable land-use management in semi-arid region. *J. Clean. Prod.* **2018**, *186*, 662–672. https://doi.org/10.1016/j.jclepro.2018.03.119.
37. Zhang, X.; Zhu, W.; Yan, N.; Wei, P.; Zhao, Y.; Zhao, H.; Zhu, L. Research on service value and adaptability zoning of grassland ecosystem in ethiopia. *Remote Sens.* **2022**, *14*, 2722. https://doi.org/10.3390/rs14112722.
38. Phan, T.; Kuch, V.; Lehnert, L. Land Cover Classification Using Google Earth Engine and Random Forest Classifier—The Role of Image Composition. *Remote Sens*. **2020**, *12*, 2411. https://doi.org/10.3390/rs12152411.
39. Rummell, A.; Leon, J.; Borland, H.; Elliott, B.; Gilby, B.; Henderson, C.J.; Olds, A.D. Watching the Saltmarsh Grow: A High-Resolution Remote Sensing Approach to Quantify the Effects of Wetland Restoration. *Remote Sens*. **2022**, *14*, 4559. https://doi.org/10.3390/rs14184559.
40. Tang, W.; Hu, J.; Zhang, H.; Wu, P.; He, H. Kappa coefficient: A popular measure of rater agreement. Shanghai Arch Psychiatry **2015**, *27*, 62–67. https://doi.org/10.11919/j.issn.1002-0829.215010.
41. Jiang, Y.; Huang, M.; Chen, X.; Wang, Z.; Xiao, L.; Xu, K.; Zhang, S.; Wang, M.; Xu, Z.; Shi, Z. Identification and risk prediction of potentially contaminated sites in the yangtze river delta. *Sci. Total Environ.* **2022**, *815*, 151982. https://doi.org/10.1016/j.scitotenv.2021.151982.
42. Zhai, H.; Lv, C.; Liu, W.; Yang, C.; Fan, D.; Wang, Z.; Guan, Q. Understanding spatio-temporal patterns of land use/land cover change under urbanization in wuhan, China, 2000–2019. *Remote Sens.* **2021**, *13*, 3331. https://doi.org/10.3390/rs13163331.
43. Saaty, T.L. A scaling method for priorities in hierarchical structures. *J. MathPsychol.* **1977**, *15*, 234–281.
44. Hu, X.; Ma, C.; Huang, P.; Guo, X. Ecological vulnerability assessment based on ahp-psr method and analysis of its single parameter sensitivity and spatial autocorrelation for ecological protection? A case of weifang city, China. *Ecol. Indic.* **2021**, *125*, 107464. https://doi.org/10.1016/j.ecolind.2021.107464.
45. Li, C.; Wu, Y.; Gao, B.; Zheng, K.; Wu, Y.; Li, C. Multi-scenario simulation of ecosystem service value for optimization of land use in the sichuan-yunnan ecological barrier, China. *Ecol. Indic.* **2021**, *132*, 108328. https://doi.org/10.1016/j.ecolind.2021.108328.
46. Fu, J.; Zhang, Q.; Wang, P.; Zhang, L.; Tian, Y.; Li, X. Spatio-temporal changes in ecosystem service value and its coordinated development with economy: A case study in hainan province, China. *Remote Sens.* **2022**, *14*, 970. https://doi.org/10.3390/rs14040970.
47. Ye, Y.; Bryan, B.A.; Zhang, J.; Connor, J.D.; Chen, L.; Qin, Z.; He, M. Changes in land-use and ecosystem services in the guang-zhou-foshan metropolitan area, China from 1990 to 2010: Implications for sustainability under rapid urbanization. *Ecol. Indic.* **2018**, *93*, 930–941. https://doi.org/10.1016/j.ecolind.2018.05.031.
48. Unwin, D.; Unwin, A. Local indicators of spatial association-foreword. *J. R. Stat. Soc. Ser. Stat.* **1998**, *47*, 413–413. https://doi.org/10.1111/1467-9884.00142.

49. Hu, H.B.; Liu, H.Y.; Hao, J.F.; An, J. Spatio-temporal variation in the value of ecosystem services and its response to land use intensity. *Acta Ecol. Sin.* **2013**, *33*, 2565–2576.
50. Ye, H.; Chen, S.; Sheng, F.; Chen, H. Research on dynamic changes of land cover and its correlation with groundwater in the shule river basin. *J. Hydraul. Eng.* **2013**, *44*, 83–90. https://doi.org/10.13243/j.cnki.slxb.2013.01.002.
51. Favretto, N.; Luedeling, E.; Stringer, L.C.; Dougill, A.J. Valuing ecosystem services in semi-arid rangelands through stochastic simulation. *Land Degrad. Dev.* **2017**, *28*, 65–73. https://doi.org/10.1002/ldr.2590.
52. Zhang, X.; Zhang, Y.; Qi, J.; Wang, Q. Evaluation of the stability and suitable scale of an oasis irrigation district in northwest China. *Water* **2020**, *12*, 2837. https://doi.org/10.3390/w12102837.
53. Yang, G.; Li, F.; Chen, D.; He, X.; Xue, L.; Long, A. Assessment of changes in oasis scale and water management in the arid manas river basin, north western China. *Sci. Total Environ.* **2019**, *691*, 506–515. https://doi.org/10.1016/j.scitotenv.2019.07.143.
54. Water Resource Department of Gansu Province. *Comprehensive planning of rational use of water resource and protection of ecosystem services in the dunhuang region*; Gansu People's Publishing House Press: Lanzhou, China, 2011.
55. Zhang, X.; Zhang, L.; He, C.; Li, J.; Jiang, Y.; Ma, L. Quantifying the impacts of land use/land cover change on groundwater depletion in northwestern China—A case study of the dunhuang oasis. *Agric. Water Manag.* **2014**, *146*, 270–279. https://doi.org/10.1016/j.agwat.2014.08.017.
56. Department of Geoscience, Chinese Academy of Sciences. *Water Resource Survey Report in Arid Regions of Northwest China*; advances in earth science: Beijing, China, 1990; Volume 11.
57. Bie, Q.; Xie, Y. The constraints and driving forces of oasis development in arid region: A case study of the hexi corridor in northwest China. *Sci. Rep.* **2020**, *10*, 17708. https://doi.org/10.1038/s41598-020-74930-z.
58. Liu, X.; Chen, X.; Hua, K.; Wang, Y.; Wang, P.; Han, X.; Ye, J.; Wen, S. Effects of land use change on ecosystem services in arid area ecological migration. *Chin. Geogr. Sci.* **2018**, *28*, 894–906. https://doi.org/10.1007/s11769-018-0971-5.
59. Zhang, H.; Yu, J.; Wang, P.; Wang, T.; Li, Y. Groundwater-fed oasis in arid northwest China: Insights into hydrological and hydrochemical processes. *J. Hydrol.* **2021**, *597*, 126154. https://doi.org/10.1016/j.jhydrol.2021.126154.
60. Zhou, D.; Wang, X.; Shi, M. Human driving forces of oasis expansion in northwestern China during the last decade-a case study of the heihe river basin. *Land Degrad. Dev.* **2017**, *28*, 412–420. https://doi.org/10.1002/ldr.2563.
61. Song, W.; Deng, X. Land-use/land-cover change and ecosystem service provision in China. *Sci. Total Environ.* **2017**, *576*, 705–719. https://doi.org/10.1016/j.scitotenv.2016.07.078.
62. Zeng, J.; Chen, T.; Yao, X.; Chen, W. Do protected areas improve ecosystem services? a case study of hoh xil nature reserve in Qinghai-Tibetan Plateau. *Remote Sens.* **2020**, *12*, 471. https://doi.org/10.3390/rs12030471.
63. Zhao, D.; Xiao, M.; Huang, C.; Liang, Y.; Yang, Z. Land use scenario simulation and ecosystem service management for different regional development models of the beibu gulf area, China. *Remote Sens.* **2021**, *13*, 3161. https://doi.org/10.3390/rs13163161.